AAC Journals.ASM.org

Characterization of a Conjugate between Rose Bengal and Chitosan for Targeted Antibiofilm and Tissue Stabilization Effects as a Potential Treatment of Infected Dentin

Annie Shrestha,[a] Michael R. Hamblin,[b,c,d] and Anil Kishen[a]

Discipline of Endodontics, Dental Research Institute, Faculty of Dentistry, University of Toronto, Toronto, Ontario, Canada[a]; Wellman Center for Photomedicine, Massachusetts General Hospital, Boston, Massachusetts, USA[b]; Department of Dermatology, Harvard Medical School, Boston, Massachusetts, USA[c]; and Harvard-MIT Division of Health Sciences and Technology, Cambridge, Massachusetts, USA[d]

Bacterial biofilms and dentin structural changes are some of the major challenges in the management of infected dentin tissue. This study characterized a photosensitizer-conjugated chitosan with enhanced photodynamic efficacy against dental biofilms, as well as the ability to reinforce the postinfected dentin matrix in order to improve its mechanical and chemical stability. Rose Bengal-conjugated chitosan (CSRB) was synthesized using a chemical cross-linking method and characterized for photophysical, photobiological, and cytotoxicity properties. Its potential as an antibacterial and matrix-reinforcing agent on dentin collagen was also evaluated. *Enterococcus faecalis* as planktonic and *in vitro* biofilms was treated with CSRB and photodynamically activated with 5 to 60 J/cm^2 green light. Dentin collagen was used for the CSRB cross-linking experiments and evaluated for chemical changes, resistance to enzymatic degradation, and mechanical properties. CSRB was a photosensitizer with efficient singlet oxygen yield. *In vitro* photoactivation gave higher fibroblast cell survival than did RB alone. CSRB showed significant antibiofilm photoinactivation ($P < 0.01$). The CSRB-cross-linked dentin collagen showed higher resistance to collagenase degradation and superior mechanical properties ($P < 0.05$). In summary, the photoactivated CSRB particles synthesized in this study may be a synergistic multifunctional treatment approach with lower cytotoxicity and effective antibiofilm activity as well as the ability to reinforce the dentin collagen to enhance resistance to degradation and improve mechanical properties. This may be a targeted treatment strategy to deal with infected dentin hard tissues in a clinical scenario, where both disinfection and structural integrity need to be addressed concomitantly.

Bacterial biofilms and dentin structural changes are major challenges in the management of infected dentin tissue. Antimicrobials are traditionally used for noninvasive management of infected hard tissue. Although chemical-based disinfectants are important to reduce microbial loads and remove infected smear layer from root dentin, they have only a limited ability to eliminate biofilm bacteria, especially from root dentinal complexities (8, 28). The chemical treatment of root dentin is known to produce irreversible hard tissue alterations, such as demineralization or surface degradation (29). The combination of ultrasonic agitation with chemical irrigants further increased the degree of surface degradation on root dentin (9). In addition, degradation of the dentin matrix is also caused by host and bacterial proteases (14). Therefore, pathologically and iatrogenically modified dentin may compromise the mechanical integrity of bulk dentin (22). The search for alternative antimicrobial approaches able to achieve effective biofilm elimination from root dentin has received considerable interest in recent times.

Photodynamic therapy (PDT) in under investigation for various purposes such as antimicrobial disinfection (15, 18), anticancer therapy (19), and tissue welding and tissue engineering approaches (6, 45). The combination of an effective photosensitizer, the appropriate wavelength of light, and ambient oxygen is the key factor in PDT (18). The singlet oxygen generated during the interaction of these three factors has been reported to have a broad range of antibacterial activity. The chances of developing microbial resistance to PDT are low, as the oxygen-based free radicals act on multiple targets within the bacterial cell (15, 18, 36). Photodynamic inactivation of a wide variety of both Gram-positive and Gram-negative species in both planktonic and biofilm forms has been reported in the literature (12, 15, 16, 36). We had previously shown that modifying a photosensitizer with a cationic polymer resulted in much better photodynamic killing of bacterial biofilms than that with either the xanthene dye Rose Bengal (RB) or the phenothiazinium dye methylene blue (36). Tissue-specific optimization of PDT using modified methylene blue delivery medium improved elimination of bacterial biofilms from root canals (16). A single-step treatment to achieve effective biofilm elimination as well as to stabilize dentin tissue would provide an excellent strategy in the management of infected root dentin. Modifying photosensitizers with bioactive polymers appears as an attractive option to achieve this objective. Immobilization of photosensitizers on polymeric supports avoids the problem of removing residual photosensitizers and provides advantages of reduced toxicity and improved stability in physiologic environments (4, 26, 41). Although photosensitizers have been conjugated with various readily available synthetic polymers, biocompatibility becomes a significant limiting factor when applied *in vivo*. Use of a naturally occurring biopolymer such as chitosan has been proposed to

Received 25 April 2012 Returned for modification 21 May 2012
Accepted 18 June 2012
Published ahead of print 9 July 2012
Address correspondence to Anil Kishen, anil.kishen@dentistry.utoronto.ca.

doi:10.1128/AAC.00810-12

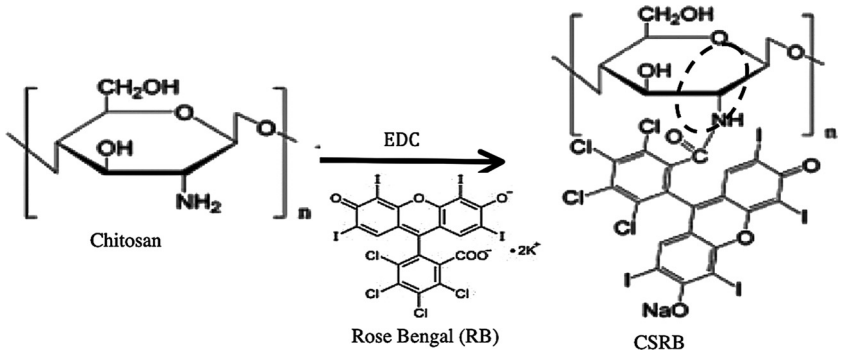

FIG 1 Schematic of the chemical reaction during conjugation of chitosan with RB in the presence of *N*-ethyl-*N*′-(3-dimethylaminopropyl)carbodiimide (EDC). The formation of chemical bonds between the NH group of chitosan and photosensitizers is highlighted with a dashed circle.

counteract the biocompatibility issues of synthetic polymers (26, 30).

Chitosan is a derivative of chitin, the second most abundant natural biopolymer, and has received significant interest in the biomedical literature (10, 47). It shows a broad range of antimicrobial activity and has biocompatible and biodegradable properties (24, 37). Chitosan has been subjected to numerous chemical modifications and grafting procedures due to its large number of free hydroxyl and amino groups (4, 24). The polymer is hydrophilic (wettable), which favors intimate contact between the photosensitizer functionalized surface and the aqueous environment of microorganisms. We formed a hypothesis that Rose Bengal-conjugated chitosan (CSRB) could perform the dual function of enhancing antibiofilm photoinactivation efficacy and improving structural stability of dentin collagen due to the synergistic effect of CSRB and singlet oxygen generated after photoactivation. In the present study, we carried out characterization of CSRB and evaluated its potential application as a dual-function antibacterial and cross-linking agent on dentin collagen. We hypothesized that CSRB could be a light-activated dual-action synergistic photosensitizer delivery vehicle that enables enhanced antibiofilm efficacy as well as the ability to induce cross-linking of collagen matrices by photoactivation.

MATERIALS AND METHODS

All the chemicals used in this study were of analytical grade and were purchased from Sigma-Aldrich (St. Louis, MO) unless noted otherwise.

Synthesis and characterization of CSRB. The CSRB was synthesized using chemical cross-linking by a carbodiimide [*N*-ethyl-*N*′-(3-dimethylaminopropyl)carbodiimide; EDC] based on a modified published protocol (26, 36). In brief, a 1% solution of chitosan was prepared in HCl (0.1 M) and stirred at room temperature in a shaker for 4 h to obtain a clear solution. After the chitosan dissolved completely, pH was increased to 5 by adding 1 M NaOH and the mixture was stirred at room temperature using a magnetic stirrer for 12 h. A solution of RB (0.05 g) was prepared in 10 ml of aqueous EDC (50 mM) and added dropwise to the chitosan solution over 30 min. The mixture was stirred for 12 h under dark conditions. The conjugated product was then dialyzed against deionized water using a dialysis membrane (Sigma; cellulose tubing; cutoff, 12,000 to 14,000 g/mol). The water was replaced daily, and dialysis was carried out for a period of 1 week. The UV-absorption spectrum (550 nm) of the deionized water used in dialysis was monitored for the presence of RB (UV-visible spectrophotometer; Shimadzu 1100; Japan). The dialysis was stopped when no RB absorption was detected in the dialysate. The polymer solution was then freeze-dried at −80°C. The CSRB powder obtained was stored in a cool and dark place until further use. The chemical structures of the reagents and product are shown in Fig. 1 (26).

Photophysical characterization of conjugated (CSRB) and unconjugated (RB) photosensitizer solutions was conducted by using UV-visible absorption spectroscopy. The ratio of monomer absorbance at 560 nm to dimer absorbance at 528 nm for different concentrations was calculated to assess aggregation in water. The effective concentration of CSRB was determined based on the highest monomer/dimer ratio. Chemical characterization of the conjugated CSRB was done using a Fourier transform infrared (FTIR) spectrophotometer (Shimadzu, Kyoto, Japan). The prepared CSRB was mixed with potassium bromide (1:100, wt/wt) to prepare pellets for the FTIR spectroscopy. The experiments were conducted in transmission mode (16-cm^{-1} resolution, 32 scans per sample).

Photo-oxidative characterization was conducted to assess the ability of CSRB to generate singlet oxygen. These experiments were conducted in 24-well plates according to a procedure described previously (17). The generation of singlet oxygen from photoactivated RB and CSRB was assessed spectrophotometrically using 1,3-diphenylisobenzofuran (DPBF), which reacts with singlet oxygen. Two milliliters of DPBF (200 μM in ethanol) was added (corresponding to an absorbance at 410 nm of 2) to 100 μl of different photosensitizer solutions. A Lumacare lamp (Lumacare Inc., Newport Beach, CA) with a 540- ± 15-nm band-pass fiber optic probe was used as a light source (power, 50 mW/cm^2). In this experiment, the rate of singlet oxygen production was related to the rate of decrease of DPBF absorbance at 410 nm (slope of linear trend line, *k* value) as a function of irradiation time. The decrease in absorbance was monitored as a function of time using a UV-visible microplate reader (Epoch; Biotek).

Evaluation of cytotoxicity and phototoxicity of CSRB. The cytotoxicity of CSRB was assessed quantitatively using a mitochondrial activity assay (spectroscopic) and qualitatively using a trypan blue exclusion assay (light microscopic). Approximately 1×10^5 NIH 3T3 mouse fibroblast cells (American Type Culture Collection, Manassas, VA; CCL 1) were seeded into 24-well plates in Dulbecco's modified Eagle's medium (DMEM) supplemented with 10% fetal bovine serum and antibiotics and incubated for 48 h in a 5% CO_2 incubator (Thermo Scientific, Waltham, MA). After incubation, the cells were treated with either CSRB or RB in DMEM at 37°C for 15 min in the dark. The cells were irradiated with 540-nm light with a total fluence of 20 J/cm^2. RB and CSRB were also tested without light irradiation (dark toxicity). The cells were incubated in the medium for 24 h before evaluation for cytotoxicity.

The supernatant medium was removed without disturbing the cells and washed with 1 ml of phosphate-buffered saline (PBS). Cell survival was determined by the standard 3-(4, 5-dimethylthiazol-2-yl)-2, 5-diphenyltetrazolium bromide (MTT) assay that determines the mitochondrial activity (27). MTT was added at a concentration of 0.5 mg/ml in medium and incubated for 4 h. After the incubation period, MTT medium was removed, and 1 ml dimethyl sulfoxide was added to dissolve the insoluble

formazan crystals. The absorbance at 540 nm was measured photometrically by using a UV-visible microplate reader. Percent survival of cells was calculated based on the control samples without any treatment as 100%. All analyses were repeated three times in triplicate (total of 9 observations), and the statistical significance was analyzed by one-way analysis of variance. The fibroblasts were also subjected to a trypan blue exclusion assay to assess their morphology following treatment. Trypan blue, a vital dye, is excluded from the living cells but stains the dead cells (48). In this assay, the treated cells were washed with PBS and stained with 1 ml of 0.4% (wt/vol) trypan blue. After 5 min of incubation at room temperature, the excess dye was washed with PBS and examined by bright-field microscopy (Leica DM; IRB, Wetzlar, Germany).

Evaluation of antibacterial efficacy of CSRB. *Enterococcus faecalis* (ATCC 29212) was used to test the antibacterial efficacy of RB and CSRB in both planktonic and biofilm forms. *E. faecalis* is a Gram-positive, facultative aerobic bacterium found at a high prevalence in persistent infections following root canal treatment (31). Overnight cultures of *E. faecalis* in brain heart infusion (BHI) broth were centrifuged (3,000 rpm, 10 min) and washed with deionized water, and the optical density was adjusted to 0.7 at 600 nm (approximately 10^9 CFU/ml). Cell pellets from 1 ml of the above suspension were collected by centrifugation, treated with 1 ml of either RB (10 μM) or CSRB (0.3 mg/ml) at 37°C for 15 min, and protected from ambient light. Dark toxicity was evaluated after 15 min of sensitization with the two treatment solutions. The control group consisted of bacterial cells without any photosensitizer or light treatment. In the case of PDT, bacterial cells were centrifuged and excess photosensitizers were removed. The sensitized planktonic bacteria were irradiated using a 540-nm fiber with doses of 5 and 10 J/cm^2. After treatment, cell pellets were resuspended in sterile deionized water (1 ml) and 100 μl of the suspension was plated on freshly poured BHI agar after serial dilution. Colonies were counted after 24 h of incubation at 37°C and expressed as log CFU per ml.

In order to test the antibacterial efficacy of photosensitizers on bacterial biofilms, 7-day-old biofilms of *E. faecalis* were grown in 24-well-plates. One milliliter of overnight culture in brain heart infusion (BHI) broth was added into each well and incubated at 37°C and 100 rpm. Fresh medium was replenished every 48 h to provide a constant supply of nutrients and to remove dead bacterial cells. On the 8th day, the medium was removed from the wells, and the biofilm was carefully washed once with sterile deionized water to remove the dead cells. The biofilm was sensitized with 1 ml of RB (10 μM) or CSRB (0.3 mg/ml) at 37°C for 15 min and irradiated at different doses (20, 40, and 60 J/cm^2). Dark toxicity was evaluated after the sensitization period with the two photosensitizers. After PDT treatment, the biofilms were washed gently, 1 ml of sterile PBS was added, and the biofilms were disrupted mechanically and plated on freshly poured BHI agar following serial dilutions. Control wells were maintained in sterile PBS. Colonies were counted after 24 h of incubation at 37°C and expressed as log CFU per ml. The experiments were carried out twice in triplicate, and the mean values were calculated.

Evaluation of CSRB to induce photodynamic cross-linking of dentin collagen. Sixteen noncarious human incisors and eight bovine incisors were collected according to a protocol approved by the University of Toronto ethical guidelines committee (protocol no. 26363) and stored in 0.9% saline at 4°C until use. The bovine teeth were used for mechanical testing while the human teeth were used to assess chemical composition and enzymatic degradation. Bovine teeth were used for the mechanical test, to avoid the difficulty of obtaining freshly extracted uniformly sized human incisors and to standardize the specimens for tensile testing (46). During experiments, dentin sections of 0.5-mm thickness were prepared from either side of the root canal using a low-speed diamond-wafering blade (Buehler, Coventry, United Kingdom) under continuous water irrigation (5). The sections were further ground into dimensions of 12 by 2 by 0.5 mm (human) and 16 by 2 by 0.2 mm (bovine) using wet emery paper of grit sizes 400, 800, and 1,000 under continuous water irrigation. The dentin sections were demineralized in 1 M EDTA (pH 7.4) for 7 days. The resulting dentin collagen specimens were rinsed for 10 min in deionized water to remove residual EDTA and subsequently stored in sterile deionized water at 4°C.

Demineralized dentin collagen specimens, human ($n = 32$) and bovine ($n = 16$), were divided into four treatment groups with human ($n = 8$) and bovine ($n = 4$) giving a total of 12 samples per group: 1, control group (no treatment); 2, glutaraldehyde group (2.5%); 3, RB group (10 μM); and 4, CSRB group (0.3 mg/ml). The dentin collagen samples were cross-linked with glutaraldehyde for a period of 6 h. In photodynamic cross-linking, collagen samples were placed in a 24-well plate (area of 2 cm^2/well) and immersed in 1 ml of RB or CSRB solution for 15 min. After the sensitization period, excess RB and CSRB were removed, and the photosensitized collagen was activated with 540-nm light for 6.5 min (20 J/cm^2). Cross-linked specimens were thoroughly washed in deionized water three times, stored in a vacuum desiccator overnight, and then tested for chemical analysis. For the enzymatic degradation analysis, the specimens were lyophilized for 24 h. The bovine dentin collagen specimens were maintained in deionized water for mechanical testing and used within a week. The control group in mechanical testing included bovine dentin collagen specimens without any treatment.

Chemical characterization. The vacuum-desiccated collagen specimens were treated with liquid nitrogen, ground, and mixed with potassium bromide (1:100, wt/wt) for the FTIR spectroscopy (16-cm^{-1} resolution, 100 scans per sample).

Enzymatic degradation. Enzymatic degradation analysis was conducted to quantify the amino acid release using the ninhydrin assay as described by Mandl et al. (25). In brief, the dentin collagen specimens were subjected to enzymatic degradation using collagenase from *Clostridium histolyticum* with an activity of 125 collagen digestion units/mg solid (P/N C-0130; Sigma). Desiccated collagen specimens (5 mg) were added into 5 ml of buffer solution (50 mM HEPES containing 0.36 mM $CaCl_2$) and incubated at 37°C for 30 min. An 0.1-ml amount of collagenase enzyme (0.1 mg/ml in HEPES buffer) was added into the collagen-containing buffer solution and incubated at 37°C in an orbital incubator (100 rpm). After 1, 2, 3, 7, and 14 days of degradation, 200 μl of the solution was added into ninhydrin reagent (2 ml), mixed well, and kept in boiling water for 30 min. The containers were allowed to cool to room temperature, and 10 ml of 50% isopropanol was added. The amount of free amino acids released following degradation of collagen specimens after heating with ninhydrin was proportional to the optical absorbance (560 nm) of the solution (39). The total amounts of amino acids released from the cross-linked and non-cross-linked dentin collagen specimens were quantified using a standard curve with L-leucine.

Determination of mechanical properties. The fully hydrated bovine dentin collagen specimens from all four test groups were used for tensile testing (Instron 5544; Instron Corp., Canton, MA) with a 100-N load cell. The specimens were positioned in the loading jig by gripping the two ends (4 mm) and subjected to tensile load at a crosshead speed of 1 mm/min until failure occurred. Care was taken to keep the samples hydrated at all times during the test. The stress-strain curve per sample was plotted for all the four groups. The ultimate tensile strength and toughness were calculated using OriginPro 8.1 software (OriginLab Corporation, MA). Toughness (MPa) was represented by the area under the stress-strain curves of each collagen sample, and percent change was used to compare cross-linking of collagen before and after.

Statistics. Averages and standard deviations were collected for each group and analyzed using one-way analysis of variance (ANOVA) and the *post hoc* Tukey test to compare groups at the 95% confidence interval.

RESULTS

Characterization of CSRB. The absorption spectra obtained for CSRB displayed peaks characteristic of RB (Fig. 2A). Approximately 10 nmol of RB molecules was attached to 1 mg of chitosan. Thus, the concentration of RB in 0.3 mg/ml of CSRB was calculated to be 3 μM. The absorption bands for CSRB were broader

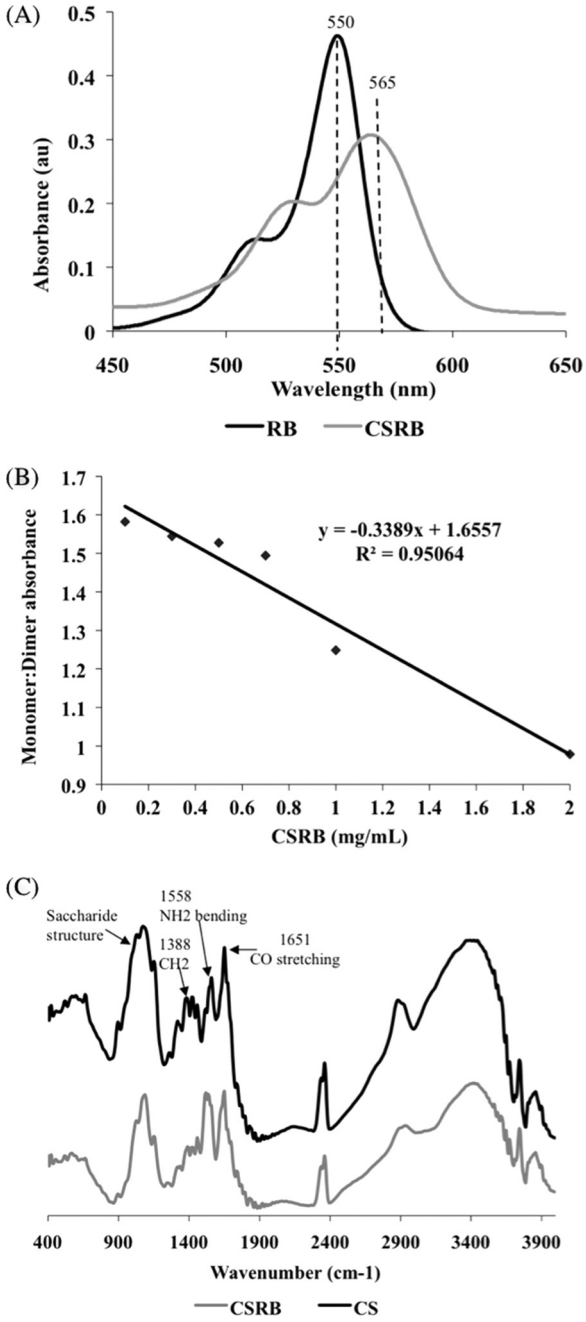

FIG 2 (A) Typical graph showing absorption spectra of RB and CSRB. The absorption peak at 549 nm of RB shifted to 560 nm and became broader following conjugation with chitosan. (B) Ratio of monomer (560-nm) to dimer (528-nm) peak decreased linearly with increase in the concentration of CSRB ($R^2 = 0.95$) in the solution, suggesting aggregation/dimerization. (C) FTIR spectra of chitosan and CSRB (400 to 4,000 cm^{-1} wave number).

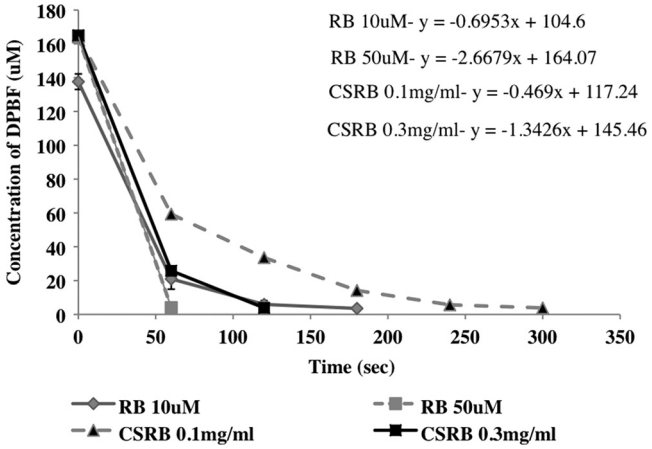

FIG 3 The oxidation of 1,3-diphenylisobenzofuran (DPBF) due to singlet oxygen generation following photoactivation of RB and CSRB measured as the reduction of DPBF absorbance.

and red-shifted compared to that of RB alone. These spectral changes confirmed that RB was attached to the polymer chain of chitosan (26). The monomer-to-dimer ratio showed a concentration-dependent response (Fig. 2B). With the increase in the concentration of CSRB, the monomer-to-dimer ratio decreased linearly. A concentration of CSRB above 0.5 mg/ml showed a dimer peak almost equal to that of monomer with a ratio near 1, indicating dimerization or aggregation. The FTIR spectra of conjugated CSRB showed bands, which could be assigned to the amide bonds between chitosan and RB (Fig. 2C). Two characteristic peaks at 1,651 (amide I, carbonyl stretching vibration) and 1,558 (NH_2 bending) cm^{-1} were prominent in chitosan and CSRB spectra (26). However, the ratio of intensities at 1,558 and 1,652 cm^{-1} was higher in CSRB than in chitosan, suggesting the reduction of amide I bonds due to utilization of the free amine groups of chitosan to form bonds with the carboxyl group of RB. The peak (900 to 1,100 cm^{-1}) corresponding to the saccharide group of chitosan was also prominent in the CSRB. The 1,388-cm^{-1} peak (-CH_2 bending) characteristic of the glucosamine units of chitosan was reduced in CSRB.

Figure 3 shows the decrease in the DPBF concentration with oxidation, which indicated the rate of singlet oxygen production upon photoactivation of CSRB and RB. It was observed that the singlet oxygen release was high enough to convert all the available DPBF for both the photosensitizers by 5 min. However, singlet oxygen release in CSRB was faster in the first 1 min, followed by a lower rate. The rate of singlet oxygen generation increased with an increase in the concentration of both the photosensitizers used. CSRB at 0.3 mg/ml ($k = 1.342$) showed a rate of production of singlet oxygen twice that of RB at 10 μM ($k = 0.695$). Based on the monomer-to-dimer ratio and singlet oxygen yield, CSRB at the concentration of 0.3 mg/ml was used in all the subsequent experiments.

Evaluation of cytotoxicity and phototoxicity of CSRB. Figure 4 shows the percent cell survival after different photosensitizer treatments under both dark and light conditions. CSRB at a lower concentration (0.3 mg/ml) showed cell survival of 75% in the dark and 48% in the light. At a higher concentration of CSRB (0.5 mg/ml), the dark toxicity was higher (60% survival) but phototoxicity was unchanged. RB showed higher dark toxicity but similar levels of phototoxicity. Under microscopic examination, cells were observed to take up CSRB into the cytoplasm (Fig. 5A), whereas RB showed aggregation at the cell membrane (Fig. 5C). Following irradiation, almost all the cells showed uptake of trypan blue. However, RB-plus-PDT-treated cells showed altered cell morphology and a dark blue nucleus (Fig. 5D) compared to the CSRB-plus-PDT-treated cells.

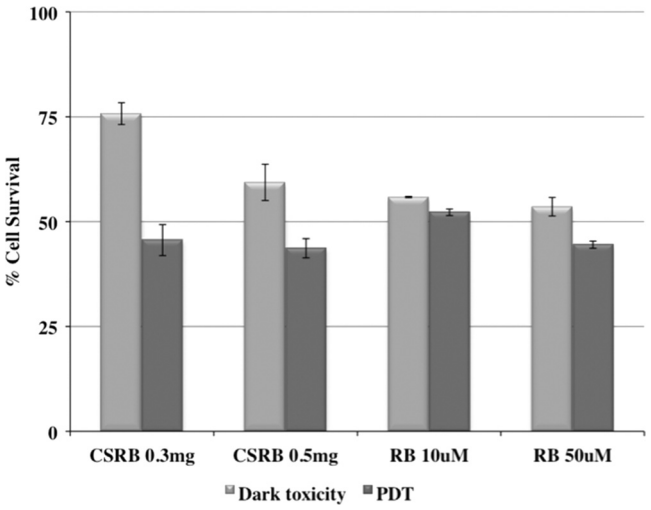

FIG 4 Graph showing cell survival following treatment with RB and CSRB with and without photodynamic treatment (PDT). PDT resulted in significantly increased cytotoxicity compared to CSRB treatment without PDT ($P < 0.05$).

CSRB-plus-PDT-treated cells showed a pinkish hue in the cytoplasm, and the morphology was maintained in most of the cells (Fig. 5B).

Evaluation of antibacterial efficacy of CSRB. Figure 6 shows the antibacterial efficacy of RB and CSRB on planktonic and biofilm bacteria under both dark and light conditions. CSRB showed a much higher level of dark killing of planktonic bacteria than did RB (Fig. 6A), as expected from the antibacterial properties of chitosan. There were more than 7 logs of killing at 0.1 mg/ml CSRB and complete eradication at 0.3 mg/ml. In contrast, RB showed dark toxicity of only an 0.5-CFU log reduction. After illumination, complete eradication was obtained with both CSRB concentrations and both fluences, while surviving bacteria were seen with RB and 5 J/cm^2.

In the case of biofilm bacteria, both CSRB and RB showed at least 3 logs of PDT-mediated bacterial killing, but in the case of CSRB, the killing was fluence dependent and was significantly higher than that by RB at 40 and 60 J/cm^2 (Fig. 6B). The biofilms with only light irradiation did not show any bacterial killing.

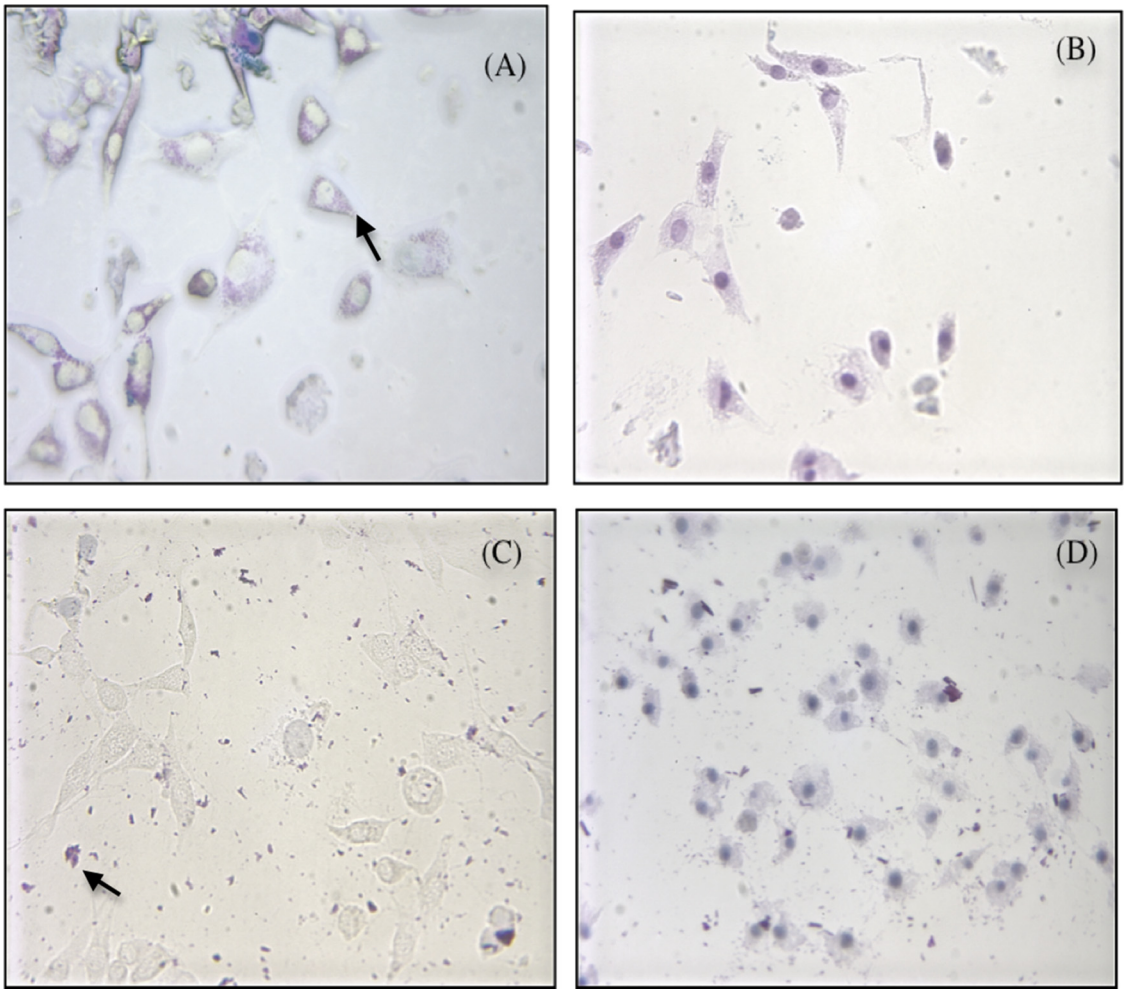

FIG 5 The trypan blue staining pattern of the cell line subjected to CSRB (A and B) and RB (C and D) treatment with and without photodynamic treatment (PDT). The cells subjected to CSRB showed the presence of photosensitizer (pink) within the cytoplasm (arrow) of the viable cells with clear round nuclei (A). RB did not show any uptake into the cells and was found outside as dark pink aggregates (arrow) (C). Following PDT, cells from both groups showed increased uptake of trypan blue uptake (nuclei of cells are stained dark bluish-purple). However, RB plus PDT (D) resulted in disruption of cell morphology and an irregular cell membrane, which was less in cells subjected to CSRB plus PDT (fibroblast cells with extensions) (B).

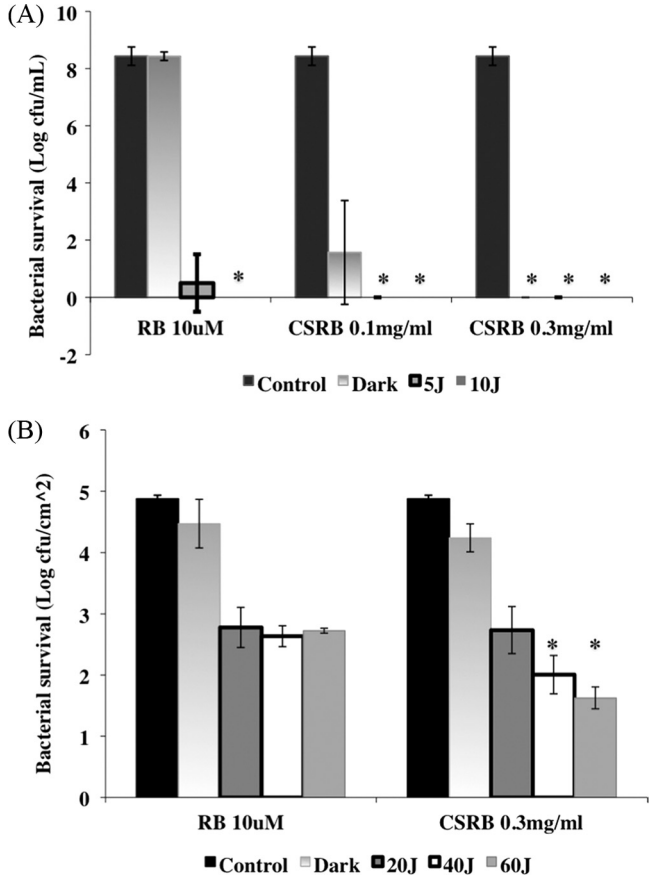

FIG 6 Log number of *E. faecalis* in planktonic (A) and biofilm (B) forms surviving the PDT conducted in a multiwell plate. There was a significant difference between the killing of biofilms by CSRB and that by RB ($P < 0.01$), as denoted by asterisks. Error bars show the standard deviations from average values.

Evaluation of CSRB to induce photodynamic cross-linking of dentin collagen. Figure 7A shows the FTIR spectra obtained from dentin collagen. The amide I bands (1,666 cm^{-1}), amide II bands (15,58 cm^{-1}), and CN bands (1,458 cm^{-1}) were analyzed to assess the presence of cross-linking (33). Amide I bands (1,666 cm^{-1}) were attributed to C═O stretching vibrations coupled to N-H bending vibration. The amide II bands (1,566 cm^{-1}) were due to the N-H bending vibrations coupled to C-N stretching vibrations (43). Following cross-linking of collagen, the amide I bands decreased compared to the amide II bands in all the cross-linked samples. The conversion of the free -NH_2 groups in collagen to N-H groups would result in a reduced amide I peak relative to the amide II peak. Cross-linking between COOH and NH_2 groups would also result in an increase in C-N bands relative to amide I bands (43).

The amounts of amino acids released following enzymatic degradation of the cross-linked and non-cross-linked dentin collagen were significantly different as a function of time ($P < 0.05$) (Fig. 7B). After 7 days, the control group specimens disintegrated nearly completely and released 9.8 μmol/ml of amino acid. Further degradation till day 14 did not show any significant increase in the amino acid release. The glutaraldehyde group showed the highest resistance to collagenase degradation even on the 14th day (0.41 μmol/ml). In the case of RB photodynamically cross-linked dentin collagen samples, resistance to degradation was comparable to that of the glutaraldehyde group till day 7 and showed a slight increase on day 14 (1.58 μmol/ml). CSRB-cross-linked dentin collagen showed a gradual increase in the release of amino acid compared to cross-linking with RB.

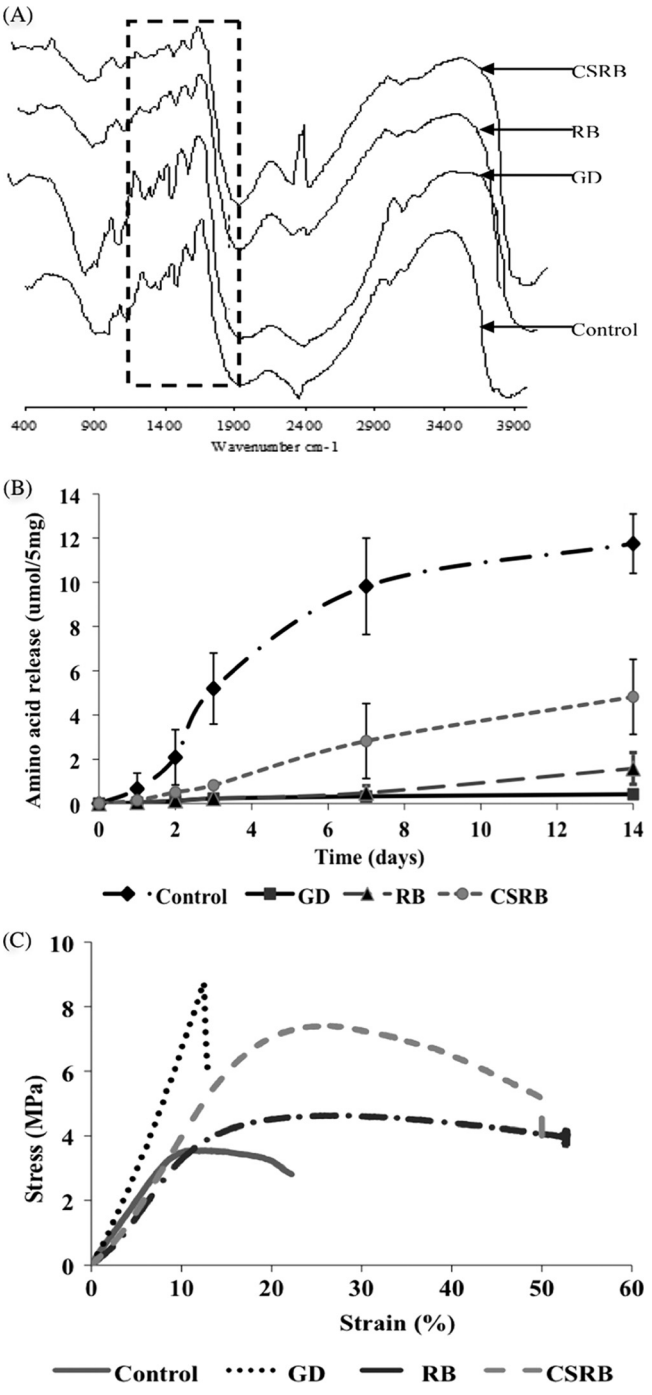

FIG 7 (A) FTIR spectra of dentin collagen; (B) amino acid released following enzymatic degradation of dentin collagen; (C) stress-strain curve after mechanical testing of dentin collagen following cross-linking. GD, glutaraldehyde.

The stress-strain curves demonstrated increased ultimate ten-

sile strength of all the cross-linked dentin collagen samples compared with the non-cross-linked control samples (Fig. 7C). The toughness was calculated for each sample as described in Materials and Methods. The glutaraldehyde-cross-linked dentin collagen samples showed a higher increase in ultimate tensile strength; however, the percent elongation of the collagen samples decreased drastically, indicating a brittle behavior. The average initial toughness of demineralized dentin collagen was 17 MPa. The glutaraldehyde cross-linking reduced toughness by almost 28% (10.74 ± 2.6 MPa). CSRB cross-linking reinforced the dentin collagen compared to the RB photo-cross-linking. The toughness of CSRB (66.67 ± 13.41 MPa) (281%)-cross-linked samples was significantly higher than that of the RB (51.95 ± 1.52 MPa) (196%)-cross-linked samples ($P < 0.05$).

DISCUSSION

Conjugation of chitosan with RB showed properties of both a bioactive polymer and a photosensitizer as determined by the FTIR and UV-visible absorption spectra of CSRB. Due to the presence of chitosan, the CSRB conjugates would be cationic in nature (abundant free amine groups). The net charge of CSRB was positive (+15 mV) but was lower than that of the unmodified chitosan particles (+20 mV) as determined previously in our lab (36). Since a higher concentration (>0.5 mg/ml) of CSRB showed aggregation as judged by the low monomer-to-dimer ratio, a concentration of 0.3 mg/ml was used in the present study. The presence of a saccharide peak in FTIR and the decreased amide I peak indicated chemical conjugation of chitosan with RB (26). Under neutral- or basic-pH conditions, chitosan with free amino groups was insoluble in water (1), but under low-pH conditions, the amino groups were protonated, thus making chitosan water soluble. Therefore, the solubility of chitosan depends on the balance between free amino and *N*-acetyl groups (1, 23). Conjugation of reactive amino groups with RB resulted in CSRB conjugate that is soluble in water (pH 7.2) (24). The ability of CSRB to produce singlet oxygen was confirmed by the indirect method of the DPBF consumption assay. The rate of singlet production by CSRB was higher than and biphasic compared to that of RB.

Increases in the uptake of photosensitizers by colorectal cancer cells following conjugation with cationic molecules have been reported in the past (11). Similarly, CSRB particles synthesized were cationic and were therefore taken up into the cytoplasm of the fibroblasts in contrast to RB, which is anionic. The biocompatibility of RB is somewhat unclear, as the dye has been described by certain groups as cytotoxic (20, 38) and by other groups as noncytotoxic (6, 7). Unmodified chitosan has been reported to favor cell growth (10, 43), and preliminary tests conducted in our lab also showed 100% fibroblast cell survival in the presence of chitosan (data not shown). In the present study, RB showed higher dark toxicity that did not increase significantly following PDT. However, the conjugation of RB with chitosan decreased the dark cytotoxicity of RB, and even after PDT, there was 50% cell survival. In another study, photosensitizer-doped conjugated polymers have been shown to show lower cytotoxicity even though they entered the cells via endocytosis (34). The polymer conjugate reduced the aggregation at the cell surface and reduced dark cytotoxicity. If CSRB were applied to decontaminate the root canal dentin, even if CSRB extruded into the apical tissues, because the fiber optic delivery system would be confined within the root canal, the amount of light energy penetrating beyond the apical foramen would be insufficient to release a harmful amount of singlet oxygen to damage apical cells. Furthermore, the presence of proteins in tissue fluids at the apical region may also lead to lessening of PDT-mediated host damage (3).

Chitosan is highly reactive toward anionic particles/surfaces such as bacteria and biofilms (32). The bacterial membrane is negatively charged owing to the lipopolysaccharide (Gram negative) and lipoteichoic acid (Gram positive) present on the surface. In the case of bacterial biofilms, the extracellular polysaccharides of the biofilm matrix are negatively charged, favoring cationic molecules to have higher binding and uptake. The hydrophilic nature of chitosan further favors the intimate binding of photosensitizer to bacterial cells. Although both chitosan and its modifications have been shown to have antibiofilm properties, they work somewhat slowly; the time taken for effective elimination was a minimum of 48 h (37). Conjugation of a photosensitizer with a positively charged molecule would allow photosensitizer molecules to enter the bacterial cells and has been shown to result in a rapid and increased killing efficiency at a lower concentration than that with the neutral and anionic photosensitizer molecules (12, 36). CSRB combined with PDT completely eliminated the biofilm bacteria, which could be due to the better uptake of photosensitizer into the bacterial cells. Subsequent photoactivation will result in the production of singlet oxygen. The slower singlet oxygen release by CSRB as seen in the biphasic pattern could provide an advantage, giving deeper penetration of singlet oxygen by not exhausting all the available ambient oxygen. The high antibacterial effect could be due to the synergistic activity of chitosan and PDT. Even though complete elimination of planktonic bacteria was observed with CSRB treatment alone, biofilm showed a much higher degree of resistance. A previous study has shown that RB could not completely eliminate biofilm bacteria (36).

The findings from this study demonstrated that cross-linking delayed the enzymatic degradation of dentin collagen and at the same time increased the overall ultimate tensile strength and fracture toughness. The chemical composition and presence of collagen cross-linking were confirmed using FTIR spectroscopy (33, 43). During PDT, the singlet oxygen produced by the activated photosensitizers is known to facilitate formation of inter- and intramolecular covalent cross-links in collagen molecules and other available reactive sites (6, 35, 38). Coupling between the free amino groups and photo-oxidized amino acids has been proven by the decrease in both reactivity and available free amino groups following photodynamic cross-linking (42). The tensile testing provided information on the mechanical properties after chemical/photodynamic cross-linking of dentin collagen (2, 41). Chitosan from the CSRB could form additional bonds with the collagen and act as spacers to prevent undesired zero-length cross-linking, subsequently reinforcing the mechanical properties (13). The bacterial collagenase enzyme degraded collagen by hydrolyzing the peptide bond on the amino-terminal side of glycine (–X-Gly-Pro) (44). Use of a commercially available purified bacterial collagenase has been used previously to degrade collagenous tissues (25, 40). Following cross-linking of collagen, the sites of collagenase attack may be hidden or modified, and this contributes to the significant difference in the release of amino acid residues following enzymatic degradation (21). Degradation of dentin collagen is a time-dependent, slow process as long as there is a fluid-tight seal. The cross-linking of dentin collagen is expected to further delay any type of degradation in

the case of interfacial leakages. In this study, untreated control specimens showed the highest overall release of amino acid at all time points in the degradation analysis.

The CSRB particles synthesized and characterized in this study may present a synergistic multifunctional treatment approach with lower cytotoxicity to effectively eliminate bacterial activity as well as the ability to cross-link and reinforce the dentin collagen matrix to enhance resistance to degradation and improve its mechanical properties. CSRB may provide a potential single-step treatment strategy to deal with infected hard tissues in a clinical scenario where both disinfection and structural integrity need to be addressed concomitantly.

ACKNOWLEDGMENTS

Funding from the University of Toronto and the Canadian Foundation of Innovation and a CIHR Training Fellowship, TGF-53877, are gratefully acknowledged. Michael R. Hamblin was supported by the U.S. NIH (grant R01AI050875).

REFERENCES

1. **Agnihotri SA, Mallikarjuna NN, Aminabhavi TM.** 2004. Recent advances on chitosan-based micro- and nanoparticles in drug delivery. J. Control. Release **100**:5–28.
2. **Bedran-Russo AK, Pashley DH, Agee K, Drummond JL, Miescke KJ.** 2008. Changes in stiffness of demineralized dentin following application of collagen crosslinkers. J. Biomed. Mater. Res. B Appl. Biomater. **86B**: 330–334.
3. **Bhatti M, MacRobert A, Meghji S, Henderson B, Wilson M.** 1997. Effect of dosimetric and physiological factors on the lethal photosensitization of Porphyromonas gingivalis in vitro. Photochem. Photobiol. **65**:1026–1031.
4. **Bonnett R, Krysteva MA, Lalov IG, Artarsky SV.** 2006. Water disinfection using photosensitizers immobilized on chitosan. Water Res. **40**: 1269–1275.
5. **Carrilho MR, et al.** 2007. In vivo preservation of the hybrid layer by chlorhexidine. J. Dent. Res. **86**:529–533.
6. **Chan BP, et al.** 2005. Photochemical repair of Achilles tendon rupture in a rat model. J. Surg. Res. **124**:274–279.
7. **Chan BP, Chan OC, So KF.** 2008. Effects of photochemical crosslinking on the microstructure of collagen and a feasibility study on controlled protein release. Acta Biomater. **4**:1627–1636.
8. **Chavez de Paz LE.** 2007. Redefining the persistent infection in root canals: possible role of biofilm communities. J. Endod. **33**:652–662.
9. **Dadresanfar B, et al.** 2011. Effect of ultrasonication with EDTA or MTAD on smear layer, debris and erosion scores. J. Oral Sci. **53**:31–36.
10. **Dasha M, Chiellini F, Ottenbrite RM, Chiellini E.** 2011. Chitosan—a versatile semi-synthetic polymer in biomedical applications. Prog. Polym. Sci. **36**:981–1014.
11. **Del Governatore M, Hamblin MR, Piccinini EE, Ugolini G, Hasan T.** 2000. Targeted photodestruction of human colon cancer cells using charged 17.1A chlorin e6 immunoconjugates. Br. J. Cancer **82**:56–64.
12. **Demidova TN, Hamblin MR.** 2005. Effect of cell-photosensitizer binding and cell density on microbial photoinactivation. Antimicrob. Agents Chemother. **49**:2329–2335.
13. **Everaerts F, et al.** 2006. Reduction of calcification of carbodiimide-processed heart valve tissue by prior blocking of amine groups with monoaldehydes. J. Heart Valve Dis. **15**:269–277.
14. **Ferrari M, Mason PN, Goracci C, Pashley DH, Tay FR.** 2004. Collagen degradation in endodontically treated teeth after clinical function. J. Dent. Res. **83**:414–419.
15. **George S, Kishen A.** 2007. Advanced noninvasive light-activated disinfection: assessment of cytotoxicity on fibroblast versus antimicrobial activity against Enterococcus faecalis. J. Endod. **33**:599–602.
16. **George S, Kishen A.** 2007. Photophysical, photochemical, and photobiological characterization of methylene blue formulations for light-activated root canal disinfection. J. Biomed. Opt. **12**:034029.
17. **Hadjur C, et al.** 1998. Spectroscopic studies of photobleaching and photo-product formation of meta(tetrahydroxyphenyl)chlorin (m-THPC) used in photodynamic therapy. The production of singlet oxygen by m-THPC. J. Photochem. Photobiol. B **45**:170–178.
18. **Hamblin MR, Hasan T.** 2004. Photodynamic therapy: a new antimicrobial approach to infectious disease? Photochem. Photobiol. Sci. **3**:436–450.
19. **Huang Z.** 2005. A review of progress in clinical photodynamic therapy. Technol. Cancer Res. Treat. **4**:283–293.
20. **Ibusuki S, et al.** 2007. Photochemically cross-linked collagen gels as three-dimensional scaffolds for tissue engineering. Tissue Eng. **13**:1995–2001.
21. **Jayakrishnan A, Jameela SR.** 1996. Glutaraldehyde as a fixative in bioprostheses and drug delivery matrices. Biomaterials **17**:471–484.
22. **Kishen A.** 2006. Mechanisms and risk factors for fracture predilection in endodontically treated teeth. Endod. Top. **13**:57–83.
23. **Kotze AF, Luessen HL, de Boer AG, Verhoef JC, Junginger HE.** 1999. Chitosan for enhanced intestinal permeability: prospects for derivatives soluble in neutral and basic environments. Eur. J. Pharm. Sci. **7**:145–151.
24. **Kumar MN, Muzzarelli RA, Muzzarelli C, Sashiwa H, Domb AJ.** 2004. Chitosan chemistry and pharmaceutical perspectives. Chem. Rev. **104**: 6017–6084.
25. **Mandl I, Maclennan JD, Howes EL.** 1953. Isolation and characterization of proteinase and collagenase from Cl. histolyticum. J. Clin. Invest. **32**: 1323–1329.
26. **Moczek L, Nowakowska M.** 2007. Novel water-soluble photosensitizers from chitosan. Biomacromolecules **8**:433–438.
27. **Mosmann T.** 1983. Rapid colorimetric assay for cellular growth and survival: application to proliferation and cytotoxicity assays. J. Immunol. Methods **65**:55–63.
28. **Nair PN, Henry S, Cano V, Vera J.** 2005. Microbial status of apical root canal system of human mandibular first molars with primary apical periodontitis after "one-visit" endodontic treatment. Oral Surg. Oral Med. Oral Pathol. Oral Radiol. Endod. **99**:231–252.
29. **Niu W, Yoshioka T, Kobayashi C, Suda H.** 2002. A scanning electron microscopic study of dentinal erosion by final irrigation with EDTA and NaOCl solutions. Int. Endod. J. **35**:934–939.
30. **Nowakowska M, Moczek L, Szczubialka K.** 2008. Photoactive modified chitosan. Biomacromolecules **9**:1631–1636.
31. **Peciuliene V, Balciuniene I, Eriksen HM, Haapasalo M.** 2000. Isolation of Enterococcus faecalis in previously root-filled canals in a Lithuanian population. J. Endod. **26**:593–595.
32. **Rabea EI, Badawy ME, Stevens CV, Smagghe G, Steurbaut W.** 2003. Chitosan as antimicrobial agent: applications and mode of action. Biomacromolecules **4**:1457–1465.
33. **Rafat M, et al.** 2008. PEG-stabilized carbodiimide crosslinked collagen-chitosan hydrogels for corneal tissue engineering. Biomaterials **29**:3960–3972.
34. **Shen X, Li L, Wu H, Yao SQ, Xu QH.** 2011. Photosensitizer-doped conjugated polymer nanoparticles for simultaneous two-photon imaging and two-photon photodynamic therapy in living cells. Nanoscale **3**:5140–5146.
35. **Shrestha A, Friedman S, Kishen A.** 2011. Photodynamically cross-linked and chitosan-incorporated dentin collagen. J. Dent. Res. **90**: 1346–1351.
36. **Shrestha A, Kishen A.** 29 November 2011. Polycationic chitosan conjugated photosensitizer for antibacterial photodynamic therapy. Photochem. Photobiol. [Epub ahead of print.] doi:10.1111/j.1751-1097.2011.01026.x.
37. **Shrestha A, Shi Z, Neoh KG, Kishen A.** 2010. Nanoparticulates for antibiofilm treatment and effect of aging on its antibacterial activity. J. Endod. **36**:1030–1035.
38. **Spikes JD, Shen HR, Kopeckova P, Kopecek J.** 1999. Photodynamic crosslinking of proteins. III. Kinetics of the FMN- and rose bengal-sensitized photooxidation and intermolecular crosslinking of model tyrosine-containing N-(2-hydroxypropyl)methacrylamide copolymers. Photochem. Photobiol. **70**:130–137.
39. **Stryer L.** 1988. Molecular basis of visual excitation. Cold Spring Harb. Symp. Quant. Biol. **53**:283–294.
40. **Sung HW, Chang Y, Liang IL, Chang WH, Chen YC.** 2000. Fixation of biological tissues with a naturally occurring crosslinking agent: fixation rate and effects of pH, temperature, and initial fixative concentration. J. Biomed. Mater. Res. **52**:77–87.
41. **Tseng SCG, Feenstra RPG, Watson BD.** 1994. Characterization of photodynamic actions of rose-bengal on cultured-cells. Invest. Ophthalmol. Vis. Sci. **35**:3295–3307.

42. **Verweij H, Dubbelman TM, Van Steveninck J.** 1981. Photodynamic protein cross-linking. Biochim. Biophys. Acta **647**:87–94.
43. **Wang XH, et al.** 2003. Crosslinked collagen/chitosan matrix for artificial livers. Biomaterials **24**:3213–3220.
44. **Watanabe K.** 2004. Collagenolytic proteases from bacteria. Appl. Microbiol. Biotechnol. **63**:520–526.
45. **Wollensak G, Iomdina E.** 2009. Long-term biomechanical properties of rabbit cornea after photodynamic collagen crosslinking. Acta Ophthalmol. **87**:48–51.
46. **Yamazaki PC, Bedran-Russo AK, Pereira PN.** 2008. The effect of load cycling on nanoleakage of deproteinized resin/dentin interfaces as a function of time. Dent. Mater. **24**:867–873.
47. **Yilmaz E.** 2004. Chitosan: a versatile biomaterial. Adv. Exp. Med. Biol. **553**:59–68.
48. **Zeina B, Greenman J, Corry D, Purcell WM.** 2002. Cytotoxic effects of antimicrobial photodynamic therapy on keratinocytes in vitro. Br. J. Dermatol. **146**:568–573.